Rf-Induced Temperature Increase in a Stratified Model of the Skin for Plane - Wave Exposure at 6-100 GHZ

Author(s):
Christ, Andreas; Samaras, Theodoros; Neufeld, Esra; Kuster, Niels

Publication date:
2020-03

Permanent link:
https://doi.org/10.3929/ethz-b-000424372

Originally published in:
Radiation Protection Dosimetry 188(3), https://doi.org/10.1093/rpd/ncz293

Radiation Protection Dosimetry (2020), Vol. 188, No. 3, pp. 350–360 doi:10.1093/rpd/ncz293
Advance Access publication 16 January 2020

RF-INDUCED TEMPERATURE INCREASE IN A STRATIFIED MODEL OF THE SKIN FOR PLANE-WAVE EXPOSURE AT 6–100 GHZ

Andreas Christ[1,*], Theodoros Samaras[2], Esra Neufeld[1] and Niels Kuster[1,3]
[1]IT'IS Foundation, Zürich, Switzerland
[2]Department of Physics, Aristotle University of Thessaloniki, Thessaloniki, Greece
[3]Swiss Federal Institute of Technology (ETHZ), Zürich, Switzerland

*Corresponding author: christ@itis.swiss

Received 1 July 2019; revised 11 November 2019; editorial decision 21 November 2019; accepted 21 November 2019

This study assesses the maximum temperature increase induced by exposure to electromagnetic fields between 6 and 100 GHz using a stratified model of the skin with four or five layers under plane wave incidence. The skin model distinguishes the stratum corneum (SC) and the viable epidermis as the outermost layers of the skin. The analysis identifies the tissue layer structures that minimize reflection and maximize the temperature increase induced by the electromagnetic field. The maximum observed temperature increase is 0.4°C for exposure at the present power density limit for the general population of 10 W m $^{-2}$. This result is more than twice as high as the findings reported in a previous study. The reasons for this difference are identified as impedance matching effects in the SC and less conservative thermal parameters. Modeling the skin as homogeneous dermis tissue can underestimate the induced temperature increase by more than a factor of three.

INTRODUCTION AND OBJECTIVES

The upcoming fifth generation of wireless communication devices will operate in an extended frequency range from 6 to 100 GHz to provide higher data rates and improved connectivity for real-time applications. The reduced penetration of the higher frequency electromagnetic (EM) energy in the human body is considered in compliance and safety guidelines issued by the ICNIRP and by IEEE TC95 [1,2], which no longer define basic restrictions in terms of the specific absorption rate (SAR). For frequencies of 10–100 GHz [1], defines reference levels for the general public of $S_{inc} = 10$ W m^{-2} averaged over 20 cm^2, where 200 W m^{-2} must not be exceeded on any 1 cm^2. According to [2], the limit for the general public of $S_{inc} = 10$ W m^{-2} is averaged over $100\lambda^2$ up to 30 GHz and 100 cm^2 at frequencies above, where a maximum of 1000 W m^{-2} must not be exceeded on any cm^2. For occupational exposures or uncontrolled environments, less conservative limits of 50 W m^{-2} [1] or 100 W m^{-2} [2] are defined.

The ICNIRP and IEEE TC95 recently provided drafts of updated guidelines [3,4] for review and comments. These guidelines propose revised limits for the exposure to EM fields at frequencies above 10 GHz and introduce a basic restriction of 20 W m^{-2} (general public) for the averaged power density that is transmitted into the tissue. The area for the averaging of the power density has the shape of a square and a size of 4 cm^2 for frequencies from 6 to <30 GHz and of 1 cm^2 at 30 GHz and above.

Several previous studies have demonstrated the impact of the tissue composition of the human body on the absorption of EM waves and have identified impedance matching and constructive interference as potential cause for increase in absorption[5–9] and temperature rise [10–12]. These studies regard the skin as a homogeneous dermis tissue with constant dielectric properties over its entire thickness. For higher frequencies up to 100 GHz, this simplification no longer appears justified because of the shorter wavelength and penetration depth. Consequently, more recent studies distinguish the unperfused epidermis layer on the skin surface for the assessment of temperature increase [13,14].

This paper presents a more detailed stratified model of the skin to extend the work of [7,8,10] to frequencies up to 100 GHz. The epidermis is represented by the viable epidermis, composed of living cells, and the stratum corneum (SC), the outermost layer of the epidermis consisting of keratinized cells[14,15]. In detail, the objectives of this study are to:

- Identify the composition of the tissue layers that maximize absorption and temperature increase for plane-wave incidence at frequencies from 6 to 100 GHz
- Quantify transmission and absorption of the incident EM energy in the layered skin model as well as the induced temperature increase in comparison to a non-layered skin model consisting of homogeneous dermis tissue only

- Assess the sensitivity of these results to changes in the anatomical, dielectric and thermal parameters of the layered skin model
- Discuss the correlation of the 1 g peak spatial average SAR (1 g psSAR) and temperature increase with the incident power density

The temperature increase is calculated for thermal equilibrium (steady state). The exposure time to reach this equilibrium depends on the thermal boundary conditions on the skin–air interface, the penetration depth of the electromagnetic fields and the anatomical tissue composition and on the shape and size on the exposed area. The discussion of all these aspects would go beyond the scope of this paper. Hence only reference to the relevant literature is made: details concerning the exposure time are discussed in[10,16–18], and the impact of the dimensions of the irradiated area and spatially inhomogeneous exposure is analyzed in[16,19,20]. Additional parameters concerning the penetration of the EM energy and the associated induced temperature increase are the angle of incidence of the fields and possible near-field coupling[21–23]. With respect to the work described here, it is relevant to mention that the temperature increase induced by EM fields in the frequency range from 6 to 100 GHz converges to the increase caused by the plane wave exposure for an irradiated surface of approximately 400 mm^2, which justifies the application of a one-dimensional model.

METHODS

Evaluation of the EM energy absorption and ΔT

As in previous studies [7,8,10], the surface layers of the body are represented by a one-dimensional sequence of tissue layers of varying thicknesses. Stratified one-dimensional models have already been used in previous studies of the absorption of EM energy at frequencies above 10 GHz [12–15,19]. Higher level anatomical details of the skin, such as the helical sweat glands, are assumed to be negligible at frequencies up to 100 GHz [24].

The body model is irradiated with a TEM-polarized plane-wave. Reflection and transmission coefficients at all tissue interfaces are calculated analytically to determine the amplitudes of the propagating and reflected waves in the layers[25]. For the calculation of the psSAR, the power density is evaluated on a discretized axis with a step size of 10 or 20 μm. The psSAR is summed up along the discretized axis considering the respective mass densities of the tissues and the length and cross section a three-dimensional cube of a mass of 1 g would have.

ΔT is then evaluated numerically on the same discretized axis by solving the steady state Pennes equation[26] through a simple matrix inversion. Details can be found, e.g. in[27]. For an efficient evaluation, both the electromagnetic and the thermal calculations are performed in a custom C++ software using the Armadillo library[28]. Post-processing of the numerical results is carried out in GNU Octave[29]. The software has been verified against the electromagnetic and thermal solvers of the simulation platform Sim4Life 4.0, ZMT Zurich MedTech AG, Switzerland.

Both adiabatic and mixed thermal boundary conditions are applied for the quantification of ΔT. Adiabatic boundary conditions assume no heat exchange between the tissue and its environment. They can be regarded as representative for situations where local heat transfer is minimized, e.g. by clothing or by a device being held against the skin. The convection cooling of uncovered skin is modeled using mixed boundary conditions. These take the ambient temperature and the heat transfer coefficient h as parameters. On the inner side of the skin model, the length of the computational mesh is chosen sufficiently long to prevent any significant impact from its termination on the distribution of the EM fields or ΔT. Since ΔT is calculated as the difference of the absolute temperatures in the tissue with and without EM heating, the ambient temperature can be disregarded, and ΔT only depends on h[30].

All results are normalized to the exposure limit $S_{inc} = 10\ W\ m^{-2}$ for the general public[1,2]. Initial investigations showed that thermoregulation or metabolism changes need not be considered in the temperature range that can be expected at this exposure level[31,32]. Hence, the model for the temperature increase is linear, and the results can readily be scaled to different exposure levels as long as these prerequisites are met.

Anatomical model of the skin

Based on the analysis of[14], the skin is represented as planar stratified structure of four or five layers of different tissues (Figure 1):

- SC: the outermost layer of the skin, consisting of unperfused keratinized cells (part of the epidermis)
- Viable epidermis: unperfused tissue with the dielectric characteristics of the dermis (part of the epidermis)
- Dermis: the outermost perfused skin layer
- Fat (hypodermis): the perfused layer consisting of subcutaneous adipose tissue (SAT)
- Muscle: the terminating layer in configurations where reflections from the fat-muscle interface are considered

In the following paragraphs, the skin model configurations with a terminating muscle layer are

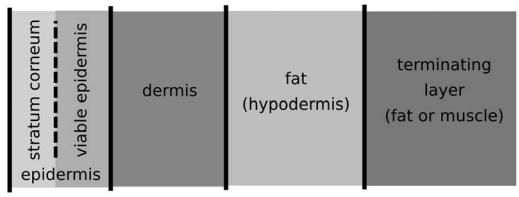

Figure 1. Model of the skin showing the sequence of the tissue layers

Table 1. Thickness ranges of the tissue layer sequences.

Tissue	Thickness range [μm]
Thick SC	20–700
Thin SC	10–20
Viable epidermis	60–120
Dermis	400–2400
Fat	1100–5600 or ∞
Muscle	∞

referred to as 'with muscle' and those with no muscle tissue and termination by the fat layer as 'without muscle.' The latter is regarded as representative for thicker fat layers where the distance to the subsequent tissue layer, such as muscle, is large enough to prevent any of the effects discussed in the results below. The thickness ranges of the tissue layers are summarized in Table 1. The two ranges of the SC are discriminated as:

- Thick SC, with a thickness range of 20–700 μm, as found in the palms and the soles of the feet
- Thin SC, with a thickness range of 10–20 μm for the remaining body regions

The upper limits of the SC reported, e.g. by [33,15], range from 280 to 480 μm only. The authors of [34–36] indicate thicknesses of up to 600–800 μm for the epidermis of the palms and up to 1.4 mm for the epidermis of the soles of the feet, attributing only a minor part of this thickness to the viable epidermis (Table 1). The actual thickness of the SC of the palms also depends on the activities of the subject and can be assumed to be much thicker for persons performing hard manual labor. Because of these considerations, an upper limit of 700 μm is assumed for the palms in this study. For the thickness of the SC in the face and the remaining regions of the body, generally values between 10 and 20 μm are reported[35–40].

The ranges of the skin tissue are chosen according to[14,34,35,41]. Following [41], the minimum thickness of the viable epidermis and the dermis can be as thin as 0.5 mm in children up to 5 years of age, whereas it lies in a range of approximately 0.8–2.4 mm for adults. Few studies also report minimum thicknesses in the order of magnitude of 0.6–0.7 mm for adults[42,43].

As mentioned above, the skin model is evaluated with and without a terminating muscle layer. In case of termination with the muscle layer, the thickness range of the fat layer is limited to 5.6 mm. At this thickness, the maximum psSAR occurs at the frequency of 6 GHz[8]. As this maximum is caused by constructive interference in the skin due to reflections at the fat-muscle interface, no further increase is expected for a larger fat layer thickness. The absence of possible cooling from the muscle layer[44] due to an excessive fat layer thickness is taken into account by terminating the skin model with fat instead of muscle. The tissue thicknesses are individually varied with a step size of 10 μm (thin SC) or 20 μm (thick SC), which leads to more than four million different configurations.

The dielectric properties of the tissues (Table 2) are taken from a one-term Cole–Cole-model of Ziskin *et al.*[14]. In part, this model is based on the traditional five-term Cole–Cole model[45] and shows only minor deviations from it in the millimeter wave frequency range. The dielectric parameters for the viable epidermis and the dermis best correspond to those of 'dry skin,' and the parameters of fat to those of 'non-infiltrated fat' of [45]. Applying the dielectric parameters of 'infiltrated fat'[45] or SAT[13] would lead to a shorter wavelength and higher attenuation in the fat layer. Enhancements of the SAR or ΔT due to constructive interference would therefore be expected to occur at a reduced thickness and to be lower in amplitude.

The thermal properties and the mass densities of the tissues are given in Table 3. They are based on the average values given in[46] for skin (dermis), infiltrated fat (fat) and muscle. As mentioned above, the SC and the viable epidermis are unperfused. Their thermal conductivity is assumed to be equal to that of the dermis. For the fat layer, the parameters of infiltrated fat are applied. At the interface of the SC to the environment, both adiabatic and mixed thermal boundary conditions are applied. As heat transfer coefficients h for the mixed boundary conditions, the authors of[47,48] report values between 2 and 7 W per m^2 per °C. A value of $h = 7$ W per m^2 per °C is used in this study in order to maximize the difference in ΔT between adiabatic and mixed boundary conditions. The impact of changes in the dielectric and thermal parameters is discussed below.

RESULTS

Absorption of the incident field energy

The absorption of EM energy of the incident field is evaluated in terms of the power transmission coefficient (Figure 2) and of the 1 g psSAR (Figure 3)

Table 2. Dielectric tissue parameters.

Frequency [GHz]	SC		Viable epidermis and dermis		Fat		Muscle		SAT	
	ε_r	σ [S m^{-1}]	ε_r	σ [S m^{-1}]	ε_r	σ [S m^{-1}]	ε_r	σ [S m^{-1}]	ε_r	σ [S m^{-1}]
6	4.36	0.12	34.4	4.0	5.25	0.29	50.5	4.3	16.0	1.6
10	4.22	0.30	31.3	8.0	4.90	0.68	45.5	10.6	14.4	3.3
15	4.01	0.57	26.8	13.8	4.42	1.21	38.2	19.5	12.3	5.6
30	3.52	1.21	16.0	27.5	3.42	2.32	21.5	39.9	8.0	10.5
40	3.33	1.44	12.1	32.6	3.10	2.68	15.6	47.1	6.6	12.1
60	3.15	1.68	8.17	37.6	2.80	3.01	9.9	54.1	5.2	13.6
80	3.08	1.78	6.49	39.8	2.68	3.15	7.5	57.0	4.7	14.2
100	3.04	1.83	5.64	40.9	2.62	3.22	6.3	58.5	4.4	14.6

SAT is only relevant for the discussion of the modified dielectric parameters.

Table 3. Thermal parameters and mass densities of the tissues.

Tissue	Thermal conductivity [W per m per °C]	Blood perfusion [W per m^3 per °C]	Density [kg m^{-3}]
SC	0.37	0	1500
Viable epidermin	0.37	0	1109
Dermis	0.37	7440	1109
Fat	0.21	1900	911
Muscle	0.49	2550	1090

for homogeneous dermis and layered tissues. For the evaluation of the 1 g psSAR in the one-dimensional tissue sequence, the dissipated power is integrated over a distance of approximately 10 mm, depending on the spatial distribution of the mass density. The penetration depth in the skin tissue at 10 GHz is 3.8 mm. The 1 g psSAR is therefore assumed to contain a significant part of the total absorbed energy. The thicknesses of the tissue layers for maximum transmission (Figure 2) are summarized in Table 4. The tissue thicknesses for the maximum 1 g psSAR are similar to those reported in Table 4.

At frequencies of up to 10 GHz, the highest transmission coefficient and the highest psSAR are observed for tissue sequences with a terminating muscle layer, due to impedance matching at the skin surface caused by reflections from the muscle layer, as previously discussed in [8,9]. At 6 GHz, the 1 g psSAR in layered tissue is about 3 dB higher than in homogeneous dermis. A reduction of the psSAR by a similar order of magnitude is observed when the muscle layer is removed.

For frequencies of 15 GHz and above, the impact of the terminating muscle layer is significantly diminished, due to both the generally lower depth of penetration at higher frequencies, which leads to merely superficial energy deposition, and to the increasing electrical conductivity in the fat tissue (Table 2) that attenuates reflections from the muscle layer and

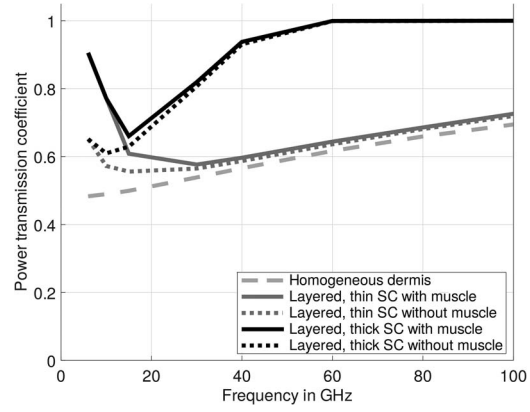

Figure 2. Maximum power transmission coefficient for homogeneous dermis and layered tissue.

prevents constructive interference. At these frequencies, the greater thickness of the SC (from 360 to 700 µm, Table 4) leads to a significant reduction of the reflection coefficient and to an increase in the 1 g psSAR of more than 1.5 dB with respect to homogeneous dermis or body regions with a SC thickness of only $\leq$20 µm.

The correlation of the 1 g psSAR with the transmitted power density (Figure 2) is given in Table 5. The proportionality coefficient c is determined by

Table 4. Tissue layer thicknesses for the transmission coefficients of Figure 2.

Freq. [GHz]	Tissue type	SC [μm]	Viable epidermis [μm]	Dermis [μm]	Fat [μm]	Muscle [μm]
6	Thin SC w. muscle	10	60	400	2860	∞
	Thin SC wo. muscle	10	60	400	∞	
	Thick SC w. muscle	20	60	400	2860	∞
	Thick SC w. muscle	20	60	400	∞	
10	Thin SC w. muscle	10	60	400	1270	∞
	Thin SC wo. muscle	20	120	2400	∞	
	Thick SC w. muscle	20	60	400	1270	∞
	Thick SC w. muscle	700	120	2400	∞	
15	Thin SC w. muscle	10	60	400	1100	∞
	Thin SC wo. muscle	20	60	1760	∞	
	Thick SC w. muscle	700	60	1660	2660	∞
	Thick SC w. muscle	700	60	1680	∞	
30	Thin SC w. muscle	20	60	1020	1580	∞
	Thin SC wo. muscle	20	60	1040	∞	
	Thick SC w. muscle	700	60	900	1600	∞
	Thick SC w. muscle	700	60	920	∞	
40	Thin SC w. muscle	20	60	830	1290	∞
	Thin SC wo. muscle	20	60	860	∞	
	Thick SC w. muscle	700	60	720	1260	∞
	Thick SC w. muscle	700	60	740	∞	
60	Thin SC w. muscle	20	60	600	1100	∞
	Thin SC wo. muscle	20	60	650	∞	
	Thick SC w. muscle	620	60	600	1100	∞
	Thick SC w. muscle	620	60	640	∞	
80	Thin SC w. muscle	20	60	520	1830	∞
	Thin SC wo. muscle	20	60	530	∞	
	Thick SC w. muscle	460	60	560	1800	∞
	Thick SC w. muscle	460	60	560	∞	
100	Thin SC w. muscle	20	60	440	1480	∞
	Thin SC wo. muscle	20	60	450	∞	
	Thick SC w. muscle	360	60	480	1520	∞
	Thick SC w. muscle	360	60	480	∞	

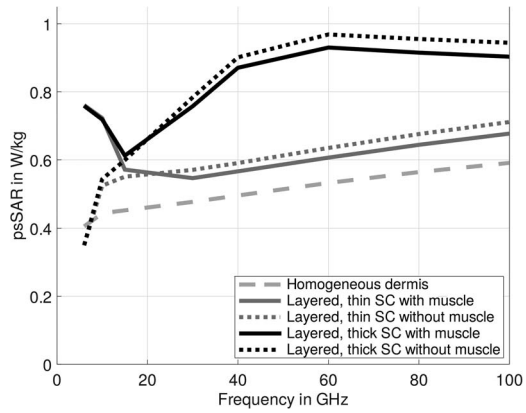

Figure 3. Maximum 1 g psSAR for homogeneous dermis and layered tissue for $S_{inc} = 10$ W m^{-2}.

linear regression with an intercept of zero, which means that the 1 g psSAR is predicted as $psSAR_{1g} = c \cdot S_{inc}$. The coefficient of determination is defined as $R^2 = 1 - SS_{res}/SS_{tot}$. SS_{res} is the sum of squares of the differences between the predicted results and the original data over the entire frequency range. SS_{tot} is the sum of squares of the difference between the original data and their mean value. Further details on linear regression can be found, e.g. in [50]. Except for the case of thin SC without muscle, the correlation is satisfactory ($R^2 > 0.75$). The poor correlation for thin SC without muscle is due to the comparatively small value of the 1 g psSAR at 6 GHz (Figure 3). It should be noted that the tissue configurations for the respective minima of the power transmission coefficient, of the 1 g psSAR maxima and of ΔT, are not always identical.

Temperature increase

Figure 4 shows the maximum ΔT for an incident power density $S_{inc} = 10$ W m^{-2} and adiabatic and mixed boundary conditions ($h = 7$ W per m^2 per °C). In homogeneous dermis tissue, ΔT increases as a function of the frequency to approximately 0.12°C

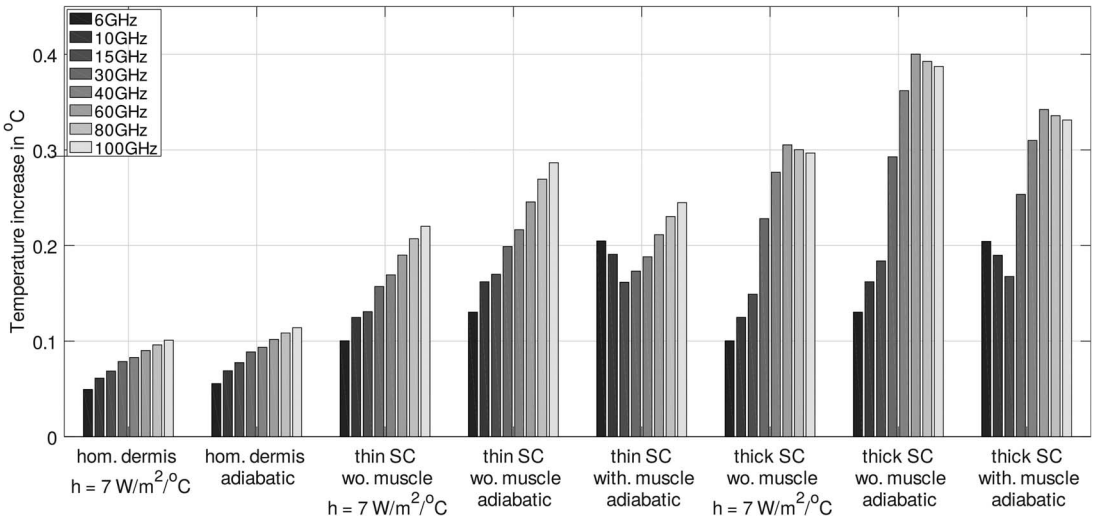

Figure 4. Maximum temperature increase for homogeneous dermis and layered tissue for $S_{\text{inc}} = 10$ W m^{-2}.

Table 5. Proportionality coefficient c of the maximum 1 g psSAR with the transmitted power density and R^2.

	c [W kg^{-1} W^{-1} m^{-2}]	R^2
Homogeneous dermis	0.087	0.96
Thin SC w. muscle	0.092	0.85
Thin SC wo. muscle	0.093	<0.5
Thick SC w. muscle	0.091	0.94
Thick SC w. muscle	0.092	0.81

at 100 GHz for adiabatic boundary conditions and to approximately 0.10°C for mixed boundary conditions. In layered tissue, the temperature increase can be more than 3-fold higher than in homogeneous dermis tissue. At 60 GHz, a maximum of 0.40°C is observed for layered tissue with thick SC, adiabatic boundary conditions and no terminating muscle layer (0.34°C for thick SC with a terminating muscle layer). Applying mixed boundary conditions reduces this increase to approximately 0.3°C (thick SC, without terminating muscle layer).

For thin SC, the maximum temperature increase (adiabatic boundary conditions, no terminating muscle layer) is approximately 0.29°C. Adding a muscle layer or mixed boundary conditions reduces this increase to 0.25 or 0.22°C, respectively. In all these cases, the maximum ΔT is observed at 100 GHz. It should be noted that these temperatures are significantly higher than the increase of approximately 0.15°C that has been reported for 100 GHz by Sasaki *et al.* [13]. The reasons for these differences are discussed in the following paragraph.

The increase of the 1 g psSAR caused by constructive interference at frequencies below 15 GHz and by impedance matching due to the higher SC thickness of the palm for the higher frequencies can be observed in a similar manner in the increase of ΔT. No such effects have been reported by Sasaki *et al.* [13]. We further observe that the absence of a terminating muscle layer leads to a greater increase in ΔT above 10 GHz, presumably because of the lower thermal conductivity and perfusion of fat tissue [44]. At 10 GHz and below, increased absorption in the dermis due to constructive interference outweighs the cooling effect of the muscle layer. The layer thicknesses for the maximum observed ΔT are summarized in Table 6.

In the frequency range from 6 to 100 GHz, the major part of the transmitted power is dissipated in the surface of the viable epidermis. Hence, the correlation of the transmitted power with the psSAR (Table 5) is better than the correlation with the temperature increase (Table 7). For the latter, the temperature spread in the tissue layers needs to be taken into account. Table 6 shows that the tissue layer thicknesses that maximize the temperature increase change significantly between 10 and 30 GHz, which further deteriorates the correlation.

The correlations of the temperature increase for adiabatic boundary conditions as a function of transmitted power density S_{trans} are given in Table 7. The proportionality coefficient d, determined by linear regression with an intercept of zero, reflects the average increase by a factor of two in the temperature of layered tissue with respect to the homogeneous dermis model. Nevertheless, the correlation is low with $R^2 < 0.75$ for most cases of layered tissue. The

Table 6. Tissue layer thicknesses for maximum temperature increase.

Freq. [GHz]	SC [μm]	Viable epidermis [μm]	Dermis [μm]	Fat [μm]	Muscle [μm]
6	20	60	400	3220	∞
10	20	60	400	5580	∞
15	700	120	1540	∞	
30	700	120	720	∞	
40	700	120	400	∞	
60	640	120	400	∞	
80	460	120	400	∞	
100	360	120	400	∞	

Table 7. Proportionality coefficient d of the maximum temperature increase with the transmitted power density and R^2.

	d [°C per W per m^2]	R^2
Homogeneous dermis	0.016	0.79
Thin SC w. muscle	0.029	<0.5
Thin SC wo. muscle	0.034	<0.5
Thick SC w. muscle	0.030	0.67
Thick SC w. muscle	0.036	0.78

findings of [10] show a consistently higher temperature increase in layered body tissue for frequencies up to 6 GHz when applying the 10 g psSAR limit and averaging mass of [1]. At frequencies above 6 GHz, the same trend toward a higher temperature can be expected as most of the transmitted power is absorbed in the outermost layers of the skin.

Modifying the dielectric and thermal parameters

The influence of changes in the dielectric properties on power transmission coefficient and ΔT is shown in Figures 5 and 6 in comparison to the peak maximum temperature increase of Figure 4 (layered, thick SC, without muscle). Replacing the dielectric parameters of the dermis by those of 'wet skin' [45] leads to a minor reduction of the power transmission coefficient at 10 GHz, but is negligible otherwise.

According to [49], the Cole–Cole parameters of 'dry skin,' which are applied to the dermis layer in this study, can be regarded as representative for the inner tissue layers, whereas the Cole–Cole parameters of 'wet' or 'moist' are based on skin tissue moistened with saline solution. As the moistening affects the skin surface, it does not apply to the inner dermis layer. Hence, 'wet skin' may only be applicable if the skin is modeled as bulk tissue. Nevertheless, it has been included here to quantify the impact of possible modeling uncertainties.

For the representation of the hypodermis, the authors of [13] use SAT, which has a higher permittivity and conductivity in comparison to the fat tissue

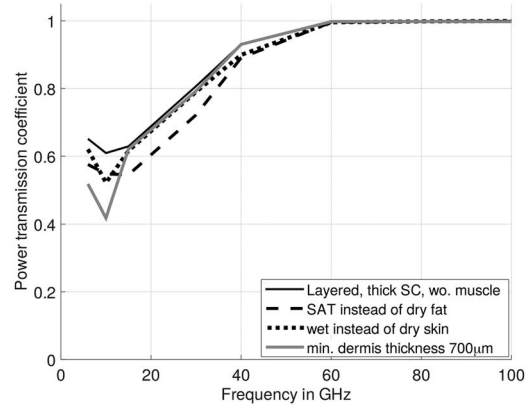

Figure 5. Impact of changes in tissue dielectrics on the power transmission coefficient for layered tissue with thick SC and without muscle (Figure 2)

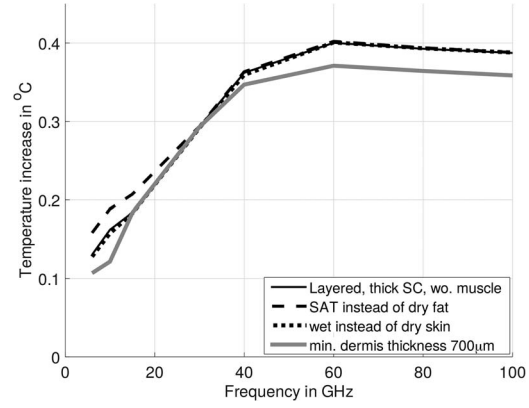

Figure 6. Impact of changes in tissue dielectrics on ΔT for the configuration with the maximum ΔT of Figure 4

applied throughout this study (Table 2). The Cole–Cole parameters for the calculation of the permittivity and conductivity of the SAT of [13] could not be retrieved. The parameters given in Table 2 are based on a reconstruction of the curves in Figure 4 of [13]

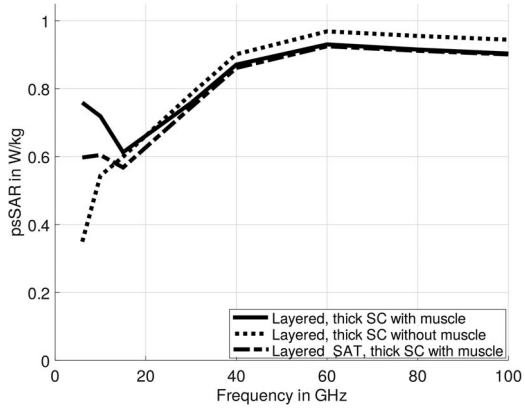

Figure 7. Impact of replacing fat by SAT on the enhancement of the 1 g psSAR due to constructive interference.

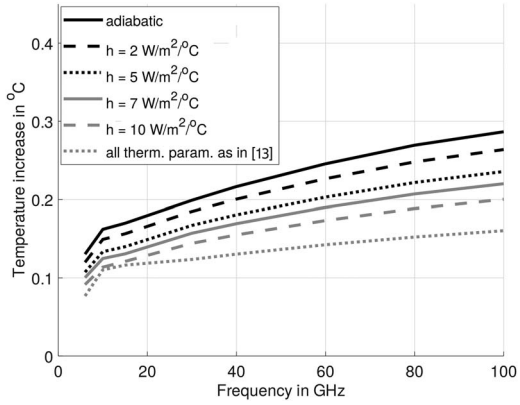

Figure 8. Impact of the heat transfer coefficient of the mixed boundary conditions on ΔT for layered tissue with thin SC (Figure 4) in comparison to adiabatic boundaries and the thermal parameters applied in [13].

and may therefore show certain deviations from the original ones. As they show a consistent increase in both permittivity and conductivity both with respect to infiltrated and non-infiltrated fat tissue [45], we are confident that they sufficiently demonstrate the impact of applying the dielectric properties of SAT to the skin model used in this study.

In the skin model without a terminating muscle layer, replacing the dielectric parameters of fat by those of SAT in the skin model used here leads to a minor reduction in the power transmission coefficient up to 40 GHz and to an increase of up to 0.03°C in ΔT for frequencies below 30 GHz. At higher frequencies, the impact of the dielectric parameters used for the hypodermis becomes negligible because of the lower penetration depth. The impact of applying the dielectric properties of SAT those of the fat layer on the constructive interference observed at 6 GHz is demonstrated by evaluating the 1 g psSAR in the skin model with muscle tissue (Figure 7). At 6 GHz, the properties of SAT lead to a drop of the 1 g psSAR of about 20% in comparison to those of fat tissue (Table 2). One gram psSAR in the skin model without muscle layer is approximately 50% below the 1 g psSAR of in the skin model with muscle, which shows that the enhancements due to constructive interference can still be observed for SAT, but that they are reduced in amplitude.

The authors of [13] apply a minimum value of approximately 0.8 mm for the sum of epidermis and dermis thickness, which corresponds to the minimum value for adults reported by [41]. Excluding the thickness range of the dermis of young children by increasing the minimum thickness of the dermis layer to 0.7 mm reduces the ΔT by approximately 0.02°C at 6 GHz and 0.03°C at 100 GHz. Between 15 and 40 GHz, no significant impact on ΔT is observed.

Figure 8 shows the dependence of ΔT on the thermal boundary conditions. As mentioned above, the authors of [47,48] report heat transfer coefficients for the mixed boundary conditions ranging from 2 to 7 W per m^2 per °C. The results presented in Figure 4 have been calculated with the upper limit of this range, i.e. with $h = 7$ W per m^2 per °C. The authors of [13] apply a heat transfer coefficient of 10 W per m^2 per °C, which leads to a ΔT of 0.20°C in comparison to a ΔT of 0.29°C for adiabatic boundary conditions at 100 GHz, which corresponds to an increase of 45%. A reduction of ΔT by 0.04°C can be observed at 100 GHz when applying the higher parameters for thermal conductivity and blood perfusion of [13] (0.42 W per m per °C and 9100 W per m^3 per °C for the dermis, 0.25 W per m per °C and 1700 W per m^3 per °C for SAT). This result is in satisfactory agreement with the ΔT originally reported by Sasaki *et al.* [13].

SUMMARY AND CONCLUSIONS

In this study, we have assessed ΔT in layered anatomical tissue induced by exposures to EM fields at frequencies between 6 and 100 GHz to determine the tissue sequences that maximize the absorption of EM energy, with a one-dimensional stratified tissue model with adiabatic and mixed thermal boundaries. The impact of the applied dielectric and thermal parameters has been quantified. In general, the values for ΔT found in this study are higher than those of previous work [13], which can be mainly attributed to the more general tissue configurations and to the thermal boundary conditions and their parameters. The results can be summarized as follows:

- At frequencies above 15 GHz, the SC acts as an impedance matching layer for the incident EM fields. Above 60 GHz, the power transmission

coefficient can reach values of almost one for SC thicknesses between 360 and 700 μm. For thin SC, no matching effects can be observed, and the power transmission coefficient reaches approximately 0.7 at 100 GHz.

- The maximum ΔT of 0.4°C for the exposure limit of $S_{inc} = 10$ W m^{-2} for the general population is observed at 60 GHz for plane wave incidence for thick SC without terminating muscle layer. The presence of the muscle layer reduces this value by approximately 15% at the upper end of the frequency range regarded in this study.
- Impedance matching does not occur for the thin SC. The maximum ΔT for $S_{inc} = 10$ W m^{-2} is 0.29°C at 100 GHz.
- Application of mixed boundary conditions with a heat transfer coefficient of 7 W per m^2 per °C can lead to a reduction of ΔT of approximately 25% in comparison to adiabatic boundary conditions.
- Modeling the skin as homogeneous dermis tissue leads to an underestimation of the induced temperature increase by more than a factor of three.
- The heterogeneous composition of skin tissue and the frequency dependence of the effects that contribute to energy absorption and temperature increase leads to unsatisfactory correlation of the 1 g psSAR or ΔT with the transmitted power density in many cases.

The results of this study can help to establish new exposure limits for the upcoming revisions of the exposure guidelines [1,2]. It should be noted that the results reported here generally exceed those of previous work. The main parameters that lead to the differences with respect to previous findings [13] are the higher thickness range of the SC as it may occur in the palm, the fingers or the soles and the less conservative thermal parameters for blood flow and thermal boundary conditions.

When the power density of the incident EM field is within the limits for the general public, the temperature increase in the body remains under 1°C. For the less conservative limits of 50 W m^{-2} for occupational exposure [1] or 100 W m^{-2} for controlled environments [2], a temperature increase of 1°C is likely to be exceeded.

For extremely localized exposures, e.g. in the vicinity of small antennas, the actual temperature increase depends on the averaging area for which the power density limits are defined. Other aspects not investigated here are the time dependence of the exposure (e.g. pulsed signals), the angle of incidence and the close near-field. Unsuitable averaging areas and limits may result in perceptible temperature increases above those caused by steady-state plane-wave exposure.

ACKNOWLEDGEMENT

The authors gratefully acknowledge the abovementioned funding and the valuable advice by Marvin Ziskin, Kenneth Foster, Quirino Balzano and Mark Douglas.

FUNDING

This work was supported by the Mobile & Wireless Forum, Merelbeke, Belgium.

REFERENCES

1. ICNIRP. *Guidelines for limiting exposure to time-varying electric, magnetic and electromagnetic fields (up to 300 GHz)*. Health Phys. **74**, 494–522 (1998).
2. IEEE C95.1. IEEE Std C95.1a IEEE Standard for Safety Levels with Respect to Human Exposure to Radio Frequency Electromagnetic Fields, 3 kHz to 300 GHz, Amendment 1: Specifies Ceiling Limits for Induced and Contact Current, Clarifies Distinctions between Localized Exposure and Spatial Peak Power Density. (3 Park Avenue, New York, NY 10016-5997, USA: IEEE Standards Department, International Committee on Electromagnetic Safety, The Institute of Electrical and Electronics Engineers, Inc.) (2010).
3. ICNIRP. *Draft guidelines for limiting exposure to time-varying electric, magnetic and electromagnetic fields (up to 300 GHz)*. submitted (2019).
4. IEEE C95.1. IEEE PC95.1/D3.3 Standard 14. for Safety Levels with Respect to Human Exposure to Radio Frequency Electromagnetic Fields, 3 kHz to 300 GHz. (3 Park Avenue, New York, NY 10016-5997, USA: IEEE Standards Department, International Committee on Electromagnetic Safety, The Institute 15. of Electrical and Electronics Engineers, Inc.) (2019).
5. Schwan, H. P. and Li, K. *Hazards due to total body irradiation*. Proc. IRE **44**, 2058–2062 (1956).
6. Meier, K., Hombach, V., Kästle, R., Tay, R. Y.-S. and Kuster, N. *The dependence of EM energy absorption upon human head modeling at 1800 MHz*. IEEE Trans. Microw. Theory Tech. **45**, 2058–2062 (1997).
7. Drossos, A., Santomaa, V. and Kuster, N. *The dependence of electromagnetic energy absorption upon human head tissue composition in the frequency range of 300–3000 MHz*. IEEE Trans. Microw. Theory Tech. **48**, 1988–1995 (2000).
8. Christ, A., Klingenböck, A., Samaras, T., Goiceanu, C. and Kuster, N. *The dependence of electromagnetic far-field absorption on body tissue composition in the frequency range from 300 MHz to 6 GHz*. IEEE Trans. Microw. Theory Tech. **54**, 2188–2195 (2006a).
9. Christ, A., Samaras, T., Klingenböck, A. and Kuster, N. *Characterization of the electromagnetic near-field absorption in layered biological tissue in the frequency range from 30 MHz to 6000 MHz*. Phys. Med. Biol. **51**, 4951–4966 (2006b).
10. Samaras, T., Christ, A., Klingenböck, A. and Kuster, N. *Worst case temperature rise in a one-dimensional*

tissue model exposed to radiofrequency radiation. IEEE Trans. Biomed. Eng. **54**, 492–496 (2007).
11. Anderson, V., Croft, R. and McIntosh, R. L. *SAR versus Sinc: What is the appropriate RF exposure metric in the range 1–10 GHz? Part I: Using planar body models*. Bioelectromagnetics **31**, 454–466 (2010).
12. Kanezaki, A., Hirata, A., Watanabe, S. and Shirai, H. *Parameter variation effects on temperature elevation in a steady-state, one-dimensional thermal model for millimeter wave exposure of one-and three-layer human tissue*. Phys. Med. Biol. **55**, 4647 (2010).
13. Sasaki, K., Mizuno, M., Wake, K. and Watanabe, S. *Monte carlo simulations of skin exposure to electromagnetic field from 10 GHz to 1 THz*. Phys. Med. Biol. **62**, 6993 (2017).
14. Ziskin, M. C., Alekseev, S. I., Foster, K. R. and Balzano, Q. *Tissue models for RF exposure evaluation at frequencies above 6 GHz*. Bioelectromagnetics **39**, 173–189 (2018).
15. Alekseev, S. and Ziskin, M. *Human skin permittivity determined by millimeter wave reflection measurements*. Bioelectromagnetics **28**, 331–339 (2007).
16. Foster, K. R., Ziskin, M. C. and Balzano, Q. *Thermal response of human skin to microwave energy: a critical review*. Health Phys. **111**, 528–541 (2016).
17. Laakso, I., Morimoto, R., Heinonen, J., Jokela, K. and Hirata, A. *Human exposure to pulsed fields in the frequency range from 6 to 100 GHz*. Phys. Med. Biol. **62**, 6980 (2017).
18. Neufeld, E. and Kuster, N. *Systematic derivation of safety limits for time-varying 5G radiofrequency exposure based on analytical models and thermal dose*. Health Phys. **115**, 705–711 (2018).
19. Hashimoto, Y., Hirata, A., Morimoto, R., Aonuma, S., Laakso, I., Jokela, K. and Foster, K. R. *On the averaging area for incident power density for human exposure limits at frequencies over 6 GHz*. Phys. Med. Biol. **62**, 3124 (2017).
20. Neufeld, E., Carrasco, E., Murbach, M., Balzano, Q., Christ, A. and Kuster, N. *Theoretical and numerical assessment of maximally allowable power-density averaging area for conservative electromagnetic exposure assessment above 6 GHz*. Bioelectromagnetics **39**, 617–630 (2018).
21. Samaras, T. and Kuster, N. *Theoretical evaluation of the power transmitted to the body as a function of angle of incidence and polarization at frequencies >6 GHz and its relevance for standardization*. Bioelectromagnetics **40**, 136–139 (2019).
22. Li, K., Sasaki, K., Watanabe, S. and Shirai, H. *Relationship between power density and surface temperature elevation for human skin exposure to electromagnetic waves with oblique incidence angle from 6 GHz to 1 THz*. Phys. Med. Biol. **64** (2019) 065016 (11pp) . doi: 065016.
23. Christ, A., Samaras, T., Neufeld, E. and Kuster, N. *Limitations of incident power density as a proxy for induced electromagnetic fields*. submitted (2019).
24. Hayut, I., Puzenko, A., Ishai, P. B., Polsman, A., Agranat, A. J. and Feldman, Y. *The helical structure of sweat ducts: their influence on the electromagnetic reflection spectrum of the skin*. IEEE Trans. Terahertz Sci. Technol. **3**, 207–215 (2013).
25. Kong, J. A. Electromagnetic Wave Theory. (Cambridge, Massachusetts, USA: EMW Publishing) (2000).
26. Pennes, H. H. *Analysis of tissue and arterial blood temperatures in the restung human forearm*. J. Appl. Physiol. **1**, 93–122 (1948).
27. Mayers, D. F. and Morton, K. W. Numerical Solutions of Partial Differential Equations: Finite Difference Methods. (Camebridge, UK: Cambridge University Press) (1994).
28. Sanderson, S. and Curtin, R. *Armadillo: a template-based C++ library for linear algebra*. J. Open Source Softw. **1**, 26 (2016).
29. Octave Community. GNU Octave 4.1.0+ (2014).
30. Yioultsis, T., Kosmanis, T., Kosmidou, E., Zygiridis, T., Kantartzis, N., Xenos, T. and Tsiboukis, T. *A comparative study of the biological effects of various mobile phone and wireless lan antennas*. IEEE Trans. Magn. **38**, 777–780 (2002).
31. Stephens, D. P., Charkoudian, N., Benevento, J. M., Johnson, J. M. and Saumet, J. L. *The influence of topical capsaicin on the local thermal control of skin blood flow in humans*. Am. J. Phys. Regul. Integr. Comp. Phys. **281**, R894–R901 (2001).
32. Kodera, S., Gomez-Tames, J. and Hirata, A. *Temperature elevation in the human brain and skin with thermoregulation during exposure to RF energy*. Biomed. Eng. Online **17**, 1 (2018).
33. Welzel, J., Reinhardt, C., Lankenau, E., Winter, C. and Wolff, H. *Changes in function and morphology of normal human skin: evaluation using optical coherence tomography*. Br. J. Dermatol. **150**, 220–225 (2004).
34. Bloom, W. and Fawcett, D. W. A Textbook of Histology. (Philadelphia: Saunders) pp. 479–509 (1968).
35. Odland, G. F. Histology and fine structure of the epidermis. In: The Skin. Helwig, E. B. and Mostofi, F. K., Eds. (Baltimore: The Williams and Wilkins) pp. 28–45 (1968).
36. Jadassohn, J. Handbuch der Haut- und Geschlechtskrankheiten Ergänzungswerk, Erster Band, 4. Teil. Vol. 1. (Springer-Verlag) (1979).
37. Blair, C. *Morphology and thickness of the human stratum corneum*. Br. J. Dermatol. **80**, 430–436 (1968).
38. Holbrook, K. A. and Odland, G. F. *Regional differences in the thickness (cell layers) of the human stratum corneum: an ultrastructural analysis*. J. Investig. Dermatol. **62**, 415–422 (1974).
39. White, M., Jenkinson, D. M. and Lloyd, D. *The effect of washing on the thickness of the stratum corneum in normal and atopic individuals*. Br. J. Dermatol. **116**, 525–530 (1987).
40. Egawa, M., Hirao, T. and Takahashi, M. *In vivo estimation of stratum corneum thickness from water concentration profiles obtained with raman spectroscopy*. Acta Derm. Venereol. **87**, 4–8 (2007).
41. Snyder, W. S., Cook, M. J., Nasset, E. S., Karhausen, L. R., Howells, G. P. and Tipton, I. H. Report of the Task Group on Reference Man. Vol. **23**, first edn. (Elsevier Science, Oxford, United Kingdom, New York, USA, Tokyo, Japan: ICRP Publication) (1975).
42. Black, M. M. *A modified radiographic method for measuring skin thickness*. Br. J. Dermatol. **81**, 661–666 (1969).
43. Dykes, P. and Marks, R. *Measurement of skin thickness: a comparison of two in vivo techniques with a conventional histometric method*. J. Investig. Dermatol. **69**, 275–278 (1977).

44. Alekseev, S. and Ziskin, M. *Influence of blood flow and millimeter wave exposure on skin temperature in different thermal models*. Bioelectromagnetics **30**, 52–58 (2009).
45. Gabriel, S., Lau, R. W. and Gabriel, C. *The dielectric properties of biological tissues: III. Parametric models for the dielectric spectrum of tissues*. Phys. Med. Biol. **41**, 2271–2293 (1996).
46. Hasgall P. A., Di Gennaro, F., Baumgärtner, C., Neufeld, E., Lloyd B., Gosselin, M. C., Payne, D., Klingenböck, A., and Kuster N. IT'ÍS database for thermal and electromagnetic parameters of biological tissues (2018) https://itis.swiss/virtual-population/tissue-properties/overview/.
47. Kurazumi, Y., Tsuchikawa, T., Ishii, J., Fukagawa, K., Yamato, Y. and Matsubara, N. *Radiative and convective heat transfer coefficients of the human body in natural convection*. Build. Environ. **43**, 2142–2153 (2008).
48. Fojtlín, M., Fišer, J. and Jícha, M. *Determination of convective and radiative heat transfer coefficients using 34-zones thermal manikin: Uncertainty and reproducibility evaluation*. Exp. Thermal Fluid Sci. **77**, 257–264 (2016).
49. Gabriel, C., Peyman, A. and Grant, E. H. *Electrical conductivity of tissue at frequencies below 1 MHz*. Phys. Med. Biol. **54**, 4863–4878 (2009).
50. Weisberg, S. Applied Linear Regression. (Hoboken, New Jersey: John Wiley & Sons, Inc.) (2005).